Afyon Kocatepe Üniversitesi Fen ve Mühendislik Bilimleri Dergisi
Afyon Kocatepe University – Journal of Science and Engineering
https://dergipark.org.tr/tr/pub/akufemubid

Araştırma Makalesi / Research Article
DOI: https://doi.org/10.35414/akufemubid.1363938
AKÜ FEMÜBİD **24** (2024) 061101 (1297-1304)
AKU J. Sci. Eng. **24** (2024) 061101 (1297-1304)

Investigation of Some Properties of 4-Amino-2-Methyl-Quinoline and CdS Nano Composite Thin Films for Production of Diodes

Makale Bilgisi / Article Info
Alındı/Received: 21.09.2023
Kabul/Accepted: 01.08.2024
Yayımlandı/Published:02.12.2024

Diyot Üretimi İçin 4-Amino-2-Metil-Kinolin ve CdS Nano Kompozit İnce Filmlerin Bazı Özelliklerinin İncelenmesi

Ramazan DEMİR[1*], İsmet KAYA[2]

[1] *Çanakkale Onsekiz Mart University, Faculty of Education, Department of Mathematics and Physics Education, Çanakkale, Türkiye*
[2] *Çanakkale Onsekiz Mart University, Faculty of Science, Department of Chemistry, Polymer Synthesis and Analysis Laboratory, Çanakkale, Türkiye*

Abstract

The aim of this study is to produce a diode, which is a basic electronic circuit element, and analyze its physical characterization. In this study, a diode was produced from CdS and $C_{10}H_{10}N_2$ films**,** and its structural, optical**,** and electrical properties were investigated. First, a thin CdS film was deposited on an ITO substrate using the CBD method. Then, a $C_{10}H_{10}N_2$ film was coated on this CdS film by the spin coating method. The CdS film has n-type semiconductor properties, whereas the $C_{10}H_{10}N_2$ film has p-type semiconductor properties. XRD, SEM, AFM, UV-Vis spectroscopy, and IV measurements were performed on the produced films. According to the XRD result, a sharp peak at 27.07° was observed in the hexagonal phase of CdS. At this angle, a grain size of 33.3 nm was calculated according to the XRD result. Based on the SEM and AFM measurement results, it was determined that the film surface was uniform and dotted. According to the UV-Vis results, in addition to the d→d* transition, π→π* and n→π* transitions were also observed. From the I-V diagram, it was seen that the heterojunction structure of the CdS/$C_{10}H_{10}N_2$ films had a diode property. The value of rectification factor was calculated as $2.91x10^2$ from the I-V data. In addition, the ideality factor was calculated as 1.93 using the traditional method.

Keywords: *Diode; CdS; 4-amino-2-methylquinoline; $C_{10}H_{10}N_2$; Thin Film*

Öz

Bu çalışmanın amacı elektronik temel devre elemanı olan bir diyot üretmek ve bununla ilgili olarak fiziksel karakterizasyonunu araştırmaktır. Yapılan bu çalışmada CdS ve $C_{10}H_{10}N_2$ filmlerinden bir diyot üretilerek yapısal, optik ve elektriksel özellikleri incelendi. İlk olarak ITO alttaş üzerine CBD yöntemiyle CdS ince filmi üretildi. Daha sonra bu CdS filmin üzerine spin coating yöntemiyle $C_{10}H_{10}N_2$ filmi kaplandı. CdS filmi n-tipi ve $C_{10}H_{10}N_2$ filmi ise p-tipi yarı iletken özelliğine sahiptir. Üretilen filmlerin XRD, SEM, AFM, UV-Vis Spektroskopi ve IV ölçümleri alındı. XRD sonucuna göre CdS'in heksagonal fazda 27,07° de keskin bir pik gözlendi. Bu açıdan tanecik büyüklüğü XRD sonucuna göre 33,3 nm olarak hesaplandı. SEM ve AFM ölçüm sonuçlarına göre düzenli ve boşluklu bir film yüzeyinin olduğu gözlendi. UV-Vis sonucuna göre d→d* geçişinin yanısıra π→π* ve n→π* geçişleri de gözlendi. I-V grafiğinden CdS/$C_{10}H_{10}N_2$ filmlerinin hetero junction yapısının diyot özelliğine sahip olduğu gözlendi. I-V verilerinden düzeltme faktörünün değeri $2.91x10^2$ olarak hesaplandı ve ilgili grafiği çizildi. Ayrıca idealite faktörü geleneksel yöntemle 1,93 olarak hesaplandı.

Anahtar Kelimeler: *Diyot; CdS; 4-amino-2-metilkinolin; $C_{10}H_{10}N_2$; İnce Film*

1. Introduction

Group II–VI semiconductor compounds have attracted great interest due to their potential applications in photovoltaic devices, photoresistors, heterojunction diodes, electroluminescent films, and surface acoustic wave devices (Farag et al., 2009). Schottky barrier diodes (SBDs) are one of the most commonly used rectifier diodes in the electronics industry. The rectifying property of metal-semiconductor diodes was first described by Schottky in the 1930s (Karataş, 2010). The most commonly studied binary II-VI compound semiconductors for photovoltaic applications are cadmium telluride (CdTe) and cadmium sulfide (CdS) thin films. Both materials have been used to develop a p-n heterojunction device structure for solar cell applications (Olusola et al., 2016).

CdS is one of the essential technological materials used as II-VI compound semiconductors due to its large direct band gap, optical absorption and good stability. The fundamental bandgap value of CdS is 2.42 eV (Ramaiah Subba Kodigala, 2001). Various methods have been used to produce CdS nanoparticles, such as chemical vapor

*Sorumlu Yazar/Corresponding Author: Ramazan Demir e-posta/e-mail: rdemir@comu.edu.tr

deposition, chemical sol-gel solution growth, ultrasonic spray pyrolysis, screen printing sintering technology, and chemical bath deposition (CBD). Among these deposition methods, the CBD technique is one of the most cost-effective and simple methods, which makes it very attractive for obtaining reproducible and uniform CdS nanoparticles. There are many potential electronic and photonic applications of CdS nanoparticles such as solar cells, photosensors, DNA sensors, and gas sensors. (Demir et al., 2012).

In recent years, much attention has been paid to the production and characterization of Schottky diodes, organic light-emitting diodes, organic field effect transistors, photovoltaics (PV), and solar cells using organic semiconductors and their derivatives due to their stability and barrier height improvement properties (Güllü et al., 2008). Organic materials have a wide range of applications in thin-film electronics. The production and characterization of the Schottky diode barrier using organic semiconductors and their derivatives has received considerable attention in recent years. Organic semiconductors can be used as active components in electronic devices. These materials offer potential advantages due to ease of processing, low cost, and large-scale device characterization. This has opened a new opportunity to replace traditional inorganic devices with organic ones (Yakuphanoglu, 2007).

The diode we produced is made of CdS and 4-amino-2-methylquinoline ($C_{10}H_{10}N_2$), which has a CAS number of 6628-04-2 and is known by various names in the literature. $C_{10}H_{10}N_2$ is a quinoline derivative, an organic compound with amine and methyl functional groups (Braun et al., 2015). $C_{10}H_{10}N_2$ is a quinoline derivative similar to naphthalene. It consists of a fused benzene ring and a pyridine ring. The geometric structure of $C_{10}H_{10}N_2$ is shown in Figure 1.

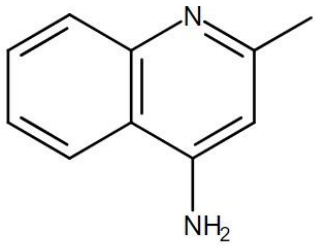

Figure 1. Structure of 4-amino-2-methyl-quinoline.

In this study, we produced a diode consisting of CdS and $C_{10}H_{10}N_2$, and investigated some physical properties of this diode. For this purpose, we prepared the CdS film using the CBD method and the $C_{10}H_{10}N_2$ film using the spin-coating method.

2. Materials and Methods

2.1. Preparation of thin films

Using the CBD method, a thin CdS film was deposited on an indium tin oxide (ITO) substrate measuring 76×26×1 mm^3. The substrates were subjected to a cleaning process that included washing with a soap solution and then rinsing with deionized water and ethanol. They were then rinsed again with deionized water and allowed to air dry. To deposit the thin CdS films, a solution was prepared consisting of 0.2 M 10 mL cadmium acetate dihydrate ($Cd(CH_3COO)_2\,2H_2O$), 1 M 10 mL thiourea ($CS(NH_2)_2$) and 8 mL ammonia/Ammonium chloride buffer solution (NH_3/NH_4Cl; pH=11.50) which was then diluted with deionized water to reach a total volume of 50 ml. To prepare the CdS film, we chose thiourea as the sulfur source (S), 82 °C as the solution temperature value, and 60 minutes as the deposition time (Demir, 2010; Demir & Gode, 2015; Demir & Göde, 2018). The CdS/ITO films accumulated in this way were then annealed in ambient air at 350 °C for 30 minutes. The chemical reactions involved in the CBD technique for producing the CdS films can be summarized as follows:

$$Cd(CH_3COO)_2\,2H_2O + N_2H_4CS \rightarrow CdS + 2CH_3COOH + H_2O + CO + N_2 + 2H_2 \quad (1)$$

The Source of $C_{10}H_{10}N_2$ was Fluka Chemika (07330, EC No. 2296044) and used in its original form. This organic compound with the chemical formula $C_{10}H_{10}N_2$ belongs to the group of heterocyclic quinoline derivatives with a methyl group at position 2 of the quinoline ring. It is commercially available as a beige powder and is also known as 4-quinolinamine and 2-methyl-4-quinolinamine. CdS is characterized as an n-type semiconductor material (Aybek A. Ş., 2018), while $C_{10}H_{10}N_2$ behaves as a p-type semiconductor material due to the same functionality as 8-hydroxyquinoline (Demir et al., 2015). $C_{10}H_{10}N_2$ has an optical band gap energy of 3.5 eV (Kaya et al., 2015).

The next phase of the experiment involved depositing a $C_{10}H_{10}N_2$ film onto a CdS film to produce a diode. To prepare the solution for the spin-coating process used to create the $C_{10}H_{10}N_2$ film, powdered $C_{10}H_{10}N_2$ with a molecular weight of 158.20 g/mol was dissolved in ethanol at room temperature for 90 minutes (22 °C). The solution concentration was 0.2 M, and the total solution volume was 30 mL. Before each rotation, 10 drops of $C_{10}H_{10}N_2$ solution were dropped onto the CdS film using a plastic dropper. The CdS film onto which a $C_{10}H_{10}N_2$ solution was dropped was attached to the spin coater.

Then, the spin coater was activated. When the spin coater stopped after 60 seconds, the produced film was left at room temperature for 5 minutes. After 5 minutes, the spin coater was activated again, and this process was repeated 8 times. For each rotation, the rotation speed of the spin coater was 1100 rpm**,** and the rotation time was 1 minute. Therefore, the previously prepared CdS film on ITO was coated with a $C_{10}H_{10}N_2$ film.

2.2. Characterization of the Thin Film's Structure

The topography, crystalline arrangement, and spectral properties of the coatings were evaluated using X-ray diffraction (XRD), UV-Vis spectroscopy, scanning electron microscopy (SEM), and atomic force microscopy (AFM), respectively.

The XRD analysis was performed using a PANalytical Empyrean instrument with λ=1.5418 Å Cu-Kα radiation within a 2θ range between 20° and 70°. The surface morphology was examined using a JEOL JSM-7100F SEM. The optical measurements of the films were carried out at room temperature using a UV-Vis spectrophotometer, specifically the Analytik Jena Specord S600, in the wavelength range between 300 and 1000 nm. The electrical characterization of the diodes was conducted using a Keithley 2400 sourcemeter under atmospheric conditions. The current-voltage characteristics of the CdS/$C_{10}H_{10}N_2$ diodes were fully characterized using a Keithley 2400 sourcemeter. The AFM measurements of the films were performed at room temperature using a WITec Alpha 300A AC mode instrument (console 42 N/m 285 kHz) to obtain topographic images. The system was enclosed in an acoustic chamber to prevent electromagnetic interference that could interfere with the measurements.

3. Results and Discussions

3.1. Composition of Thin Films

The XRD spectrum illustrating the CdS/$C_{10}H_{10}N_2$ films is depicted in Figure 2. The structural characteristics of the CdS/$C_{10}H_{10}N_2$ heterojunction were explored via XRD analysis. Table 1 presents the XRD analysis data, including information regarding crystal structure, interlayer spacing, and particle size. The Debye-Scherer equation was used to calculate the D particle size of the prepared heterojunction structures from the diffraction data.

$$D=(0.9\lambda)/(\beta.\cos\theta) \quad (2)$$

In this equation, (λ) represents the X-ray wavelength (1.5406 Å), (θ) is the Bragg diffraction angle, and (β) is the half-width of the diffraction peak (Reddy & Kumar, 2016).

Table 1. XRD parameters for CdS/$C_{10}H_{10}N_2$ pattern.

	Peak position [2θ°]	d-spacing [Å]	β (FWHM) [rad]	Grain size [nm]	Cos θ	Micro Strain (Ɛ) x 10^{-3}
	27.0774	3.2931	0.0042	33.3524	0.9722	**0.0595**
	44.3515	2.0424	0.0084	17.6519	0.9260	**0.1125**
Maximum peaks	25.5425	3.4874	0.0033	42.6482	0.9752	**0.0465**
	52.4988	1.7431	0.0074	20.8908	0.8968	**0.0950**
	67.0258	1.3963	0.0028	59.1816	0.8337	**0.0335**

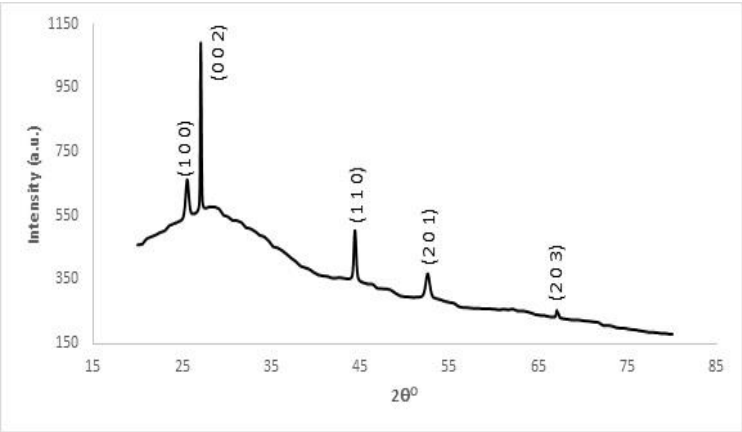

Figure 2. XRD pattern of CdS**/**$C_{10}H_{10}N_2$ sample.

The microstrain (Ɛ) was determined using the following formula (Reddy & Kumar, 2016).

$$Ɛ=(\beta.\cos\theta)/4 \quad (3)$$

Although the CdS peaks do not exactly match the standard peaks, they are close to the PDF map (greenockite, hexagonal structure) 41-1049. By comparing it with PDF Cards, it is possible to fully

understand which elements the X-ray peaks belong to. For this reason, the corresponding PDF Card number corresponding to the relevant peaks is written as in other studies (Assili et al., 2019; Demir & Gode, 2015). Interactions between CdS and $C_{10}H_{10}N_2$ cause some deviations in the actual values of this CdS film, resulting in a discrepancy between the measured and standard peaks. Figure 2 presents the XRD pattern of the thin film on the ITO substrate, revealing the hexagonal phase of CdS with lattice parameters of a=4.141 Å and c=6.719 Å. The sharp diffraction peak at 2θ=27.07° of the (002) plane indicates preferred orientation. However, the $C_{10}H_{10}N_2$ film exhibits an amorphous structure, as evidenced by the absence of any discernible peaks.

3.2. Optical Characterization

The optical measurements were carried out on the prepared films. Later, the UV-Vis spectra of the CdS film with a coating of $C_{10}H_{10}N_2$ were worked out using the "Analytik Jena Specord S600" single-beam spectrophotometer. Figure 3 shows the measured UV-Vis spectra for CdS and CdS/$C_{10}H_{10}N_2$.

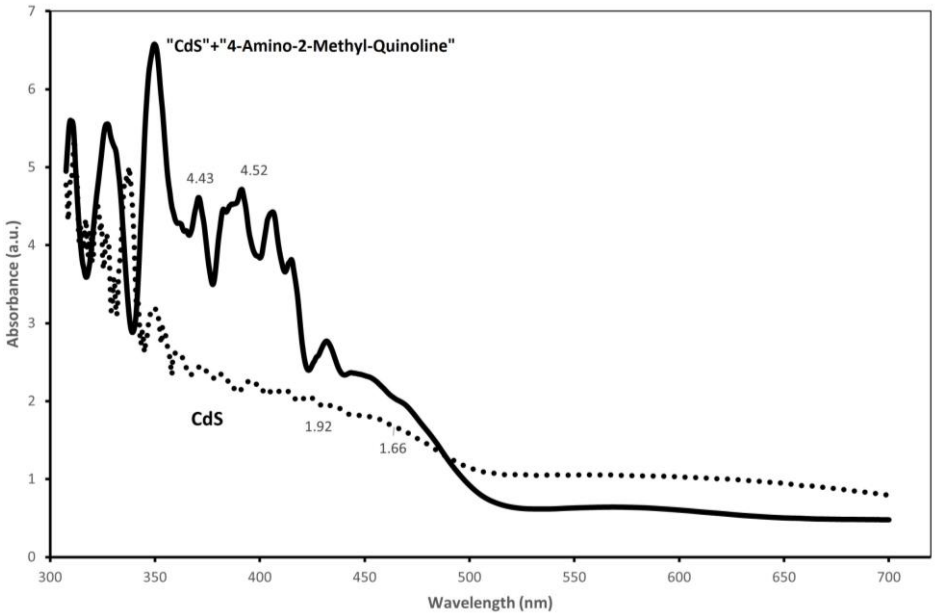

Figure 3. UV-Vis spectra of CdS and CdS/$C_{10}H_{10}N_2$

To examine the structure of the produced device, UV examination was carried out. UV-Vis spectroscopy is a cost-effective, simple**,** flexible, and non-destructive analytical method suitable for a broad class of organic compounds and some inorganic species. UV-Vis spectrophotometers measure the absorption or transmission of light passing through a medium as a function of wavelength. UV-visible spectroscopy is based on electronic transitions of organic molecules that absorb light and excite electrons from a lower energy orbital (highest occupied molecular orbital - HOMO) to a higher energy unoccupied orbital (lowest unoccupied molecular orbital - LUMO) (Rocha et al., 2018). By measuring the wavelength of these transitions, we gain insight into the nature of the transition and obtain information about the film. Based on the UV-Vis measurements, absorption bands associated with d→d* transitions of metal atoms were observed in the wavelength range of 440–500 nm. These bands indicate the presence of metal atoms within the film structure. In the CdS/$C_{10}H_{10}N_2$ films, the electronic transitions of the phenyl ring (-NH2 group) to π→π* and n→π* were observed at wavelengths of 310 nm and 328 nm, respectively.

3.3. Current-Voltage Characterization

Current-voltage (I-V) characterizations were performed on CdS**/**$C_{10}H_{10}N_2$ heterojunction structures using a two-point probe technique with a Keithley 2400 sourcemeter, as shown in Figure 4. The specialist computer software connected to the Keithley 2400 source meter recorded the current values (I) corresponding to the applied voltage (V).

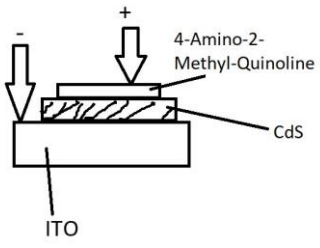

Figure 4. Measurement of current-voltage measurement of CdS**/**$C_{10}H_{10}N_2$ heterojunction structure

The current (I) was obtained by applying a direct voltage (V) ranging between -3 and 3 volts. The purpose of this study was not to investigate the photosensitivity of the heterojunction diode we produced. For this reason, I-V measurements were performed only in daylight in a laboratory environment at a laboratory temperature of 22°C. Figure 5 shows the I-V diagram of the CdS/$C_{10}H_{10}N_2$ heterojunction diode under forward and reverse bias.

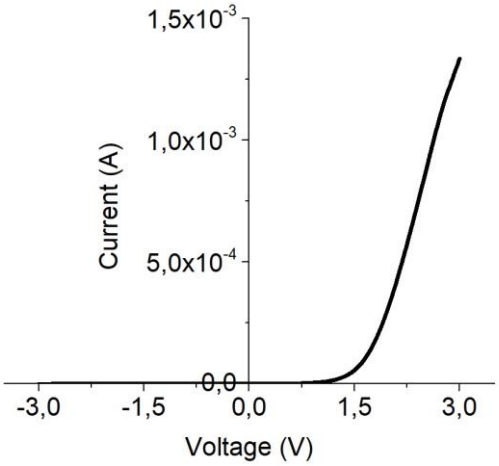

Figure 5. I-V graph of CdS/$C_{10}H_{10}N_2$ heterojunction

From Figure 5, it can be seen that the CdS/$C_{10}H_{10}N_2$ heterojunction structure exhibits diode-like characteristics in terms of current behavior and has a threshold voltage value of 1.5 volts. If there was no rectification, the graph for values between -3 and +3 volts would be the y=m.x graph.

The rectification factor (RF) is defined as the ratio of forward and reverse currents (I_F/I_R) (Kaleli et al., 2011) and is calculated as $2.91x10^2$ as a maximum value at 2.66 volts. If there was no rectification, the I_F/I_R value would be 1. The relationship between the rectification factor and the voltage at room temperature is shown in Figure 6.

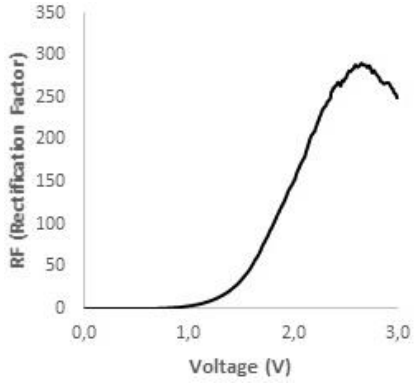

Figure 6. Plot of rectification factor (RF) versus V at room temperature.

The relationship between the voltage applied to the contact and the current flowing through a Schottky barrier is given in Equation 4, which considers the series resistance (R_S) effect. This is expressed as follows (Durmuş & Karataş, 2019; Karataş et al., 2007) :

$$I = I_0 \left[exp\left(q \frac{(V - IR_S)}{nkT} - 1 \right) \right] \quad (4)$$

The ideality factor, denoted by n, is equal to 1 for an ideal diode. The value 1 can be neglected in the equation if V > 3kT/q. T represents the ambient temperature in Kelvin, I_0 is the extrapolated saturation current, q is the elementary charge (=1.6×10^{-19} C), V is the applied voltage, and k is the Boltzmann constant.

Using Equation 4 to calculate the ideality factors of the diodes, the following expression can be obtained (Yakuphanoglu, 2007):

$$n = \frac{q}{kT} \frac{dV}{d(lnI)} \quad (5)$$

The value of the term $\frac{dV}{d(lnI)}$ in this expression is determined from the slope of the forward bias region of the *I-V* characteristic. The ideality factor n was calculated to be 1.93 using the traditional method.

3.4. SEM and AFM Analyses

The morphological features of the CdS/$C_{10}H_{10}N_2$ film were analyzed by SEM measurements, as shown in Figure 7 a–b. Charging effects induce the deflection of the incident beam and emitted secondary electrons due to the external electric field, resulting in image distortion and, in some cases, rendering their capture impossible. To prevent such false effects, various methods have been developed. One of them is the reduction of beam energy in low voltage scanning electron microscopy (LVSEM) (Cazaux, 2004). For SEM analysis, gold-palladium plating (80–20%) was performed by first applying a vacuum of 8×10^{-1} mbar/Pa and then applying a voltage of 10 mA in the Quorum coating device for 60 seconds to prevent charging on the surface of the samples and to increase the conductivity properties of the samples. The palladium layer thickness is approximately 3-4 nm. In another study by Nallathambi et al. Palladium was used as a coating material (Nallathambi et al., 2018). The SEM images show that the film surface had irregularities and did not have a periodic arrangement of the grains. The CdS/$C_{10}H_{10}N_2$ film showed an irregular and hollow structure.

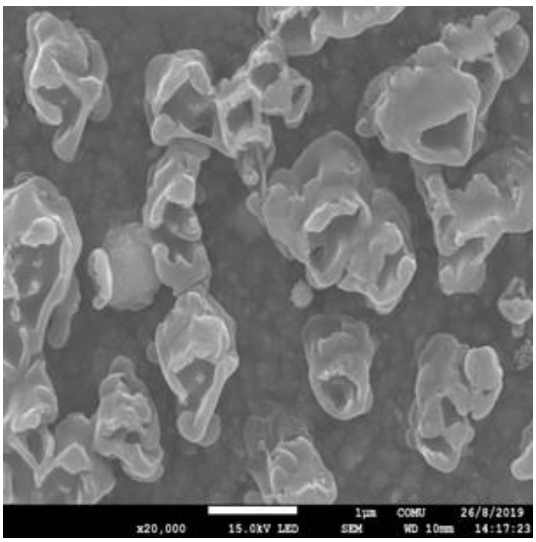

(a)

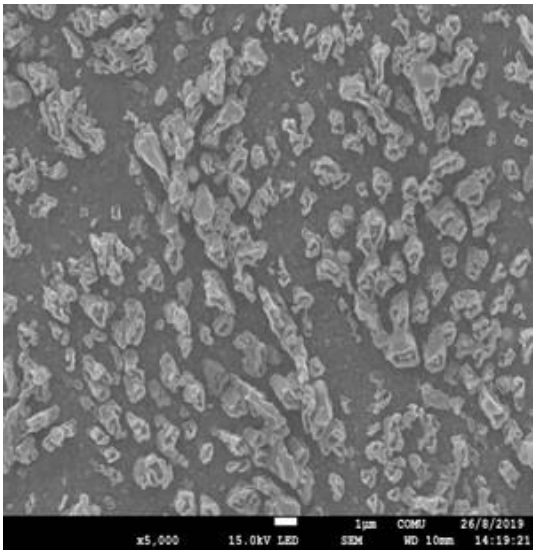

(b)

Figure 7 a-b. SEM images of CdS/$C_{10}H_{10}N_2$ film.

The AFM images of the CdS/$C_{10}H_{10}N_2$ film in three dimensions (9 µm × 9 µm) are shown in Figure 8 (a–c). These images, taken at different locations on the film, show irregularly shaped grains ranging in size from 195 nm to 240 nm.

4. Conclusion

The study began with the preparation of a CdS film on an ITO substrate using the CBD method. Then, a $C_{10}H_{10}N_2$ film was spin-coated on the CdS film to produce a diode device. Comprehensive characterization procedures, SEM, AFM, XRD, and I-V measurements were carried out. According to the SEM and AFM analyses, the CdS/$C_{10}H_{10}N_2$ film exhibited an irregular and hollow structure. The XRD results showed peaks for the CdS/$C_{10}H_{10}N_2$ films in the 2θ range of 27.00–67.00 degrees. Current-voltage measurements showed that the diode device had a threshold voltage value of 1.5 volts and conducted current in one direction with a rectification factor of 2.91×10^2, confirming its diode properties.

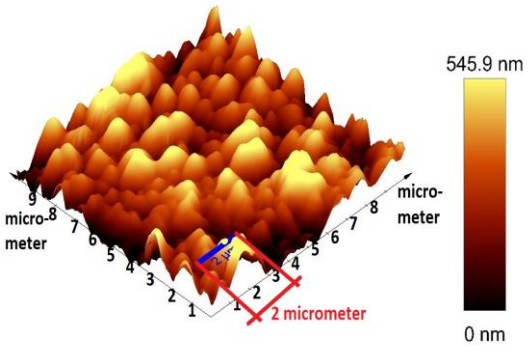

(a)

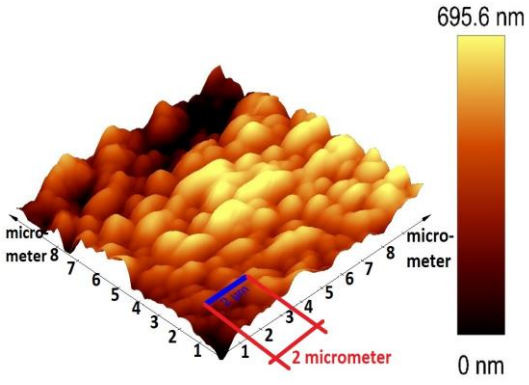

(b)

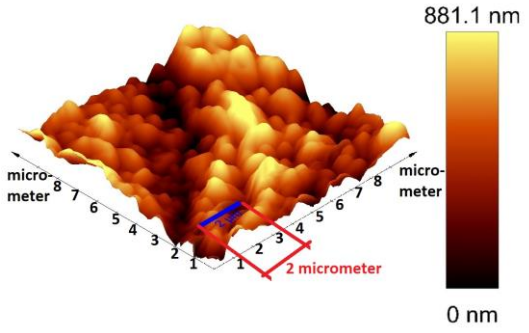

(c)

Figure 8 a-c. AFM images of CdS/$C_{10}H_{10}N_2$ film.

The n value, calculated using Equation 5, was found to be 1.93, indicating non-ideal behavior of the diode. This observation is significant as it marks the absence of prior applications of aminoquinolines as basic electronic switching elements such as diodes. Our study aimed to demonstrate the feasibility of producing a diode using the organic compound 4-amino-2-methyl-quinoline in conjunction with cadmium sulfide. By introducing this diode to the literature, we aim to provide researchers with an alternative avenue for specific studies in this domain.

Declaration of Ethical Standards
The authors declare that they comply with all ethical standards.

Credit Authorship Contribution Statement
Author-1: Conceptualization, investigation, methodology and software, visualization and writing – original draft.
Author-2: Conceptualization, investigation, methodology and software, supervision and writing – review and editing.

Declaration of Competing Interest
The authors have no conflicts of interest to declare regarding the content of this article.

Data Availability Statement
All data generated or analyzed during this study are included in this published article.

5. References

Assili, K., Selmi, W., Alouani, K., & Vilanova, X. (2019). Computational study and characteristics of In2S3 thin films: effects of substrate nature and deposition temperature. *Semiconductor Science and Technology*, *34*(4). https://doi.org/10.1088/1361-6641/ab0446

Aybek A. Ş., R. H. (2018). Some Physical Properties of FTO/n-CdS/Au Structure. *Chalcogenide Letters*, *15*, 583-590.

Braun, D. E., Gelbrich, T., Kahlenberg, V., & Griesser, U. J. (2015). Solid state forms of 4-aminoquinaldine - From void structures with and without solvent inclusion to close packing. *CrystEngComm*, *17*(12), 2504-2516. https://doi.org/10.1039/C5CE00118H

Cazaux, J. (2004). About the Mechanisms of Charging in EPMA, SEM, and ESEM with Their Time Evolution. *Microscopy and Microanalysis*, *10*, 670-684. https://doi.org/10.1017/S1431927604040619

Demir, H. Ö., Meral, K., Aydoğan, Ş., Bozgeyik, M. S., & Bayır, E. (2015). Synthesis, characterization and diode application of poly(4-(1-(2-phenylhydrazono)ethyl)phenol). *Journal of Materials Chemistry C*, *3*(22), 5803-5810. https://doi.org/10.1039/c5tc00857c

Demir, R. (2010). *The study on some physical properties of CdS thin films obtained by chemical bath deposition method* (Publication Number 269644) [Doctorate, Anadolu University, TURKEY]. Council of Higher Education Thesis Center.

Demir, R., & Gode, F. (2015). Structural, optical and electrical properties of nanocrystalline CdS thin films grown by chemical bath deposition method. *Chalcogenide Letters*, *12*, 43-50.

Demir, R., & Göde, F. (2018). Preparation and Characterization of Polycrystalline CdS Thin Films Deposited by Chemical Bath Deposition. *Materials Focus*, *7*(3), 351-355. https://doi.org/10.1166/mat.2018.1525

Demir, R., Okur, S., & Şeker, M. (2012). Electrical Characterization of CdS Nanoparticles for Humidity Sensing Applications. *Industrial & Engineering Chemistry Research*, *51*(8), 3309-3313. https://doi.org/10.1021/ie201509a

Durmuş, H., & Karataş, Ş. (2019). The analysis of the electrical characteristics and interface state densities of Re/n-type Si Schottky barrier diodes at room temperature. *International Journal of Electronics*, *106*, 507-520. https://doi.org/https://doi.org/10.1080/00207217.2018.1545145

Farag, A. A. M., Yahia, I. S., & Fadel, M. (2009). Electrical and photovoltaic characteristics of Al/n-CdS Schottky diode. *International Journal of Hydrogen Energy*, *34*(11), 4906-4913. https://doi.org/10.1016/j.ijhydene.2009.03.034

Güllü, Ö., Aydoğan, Ş., & Türüt, A. (2008). Fabrication and electrical characteristics of Schottky diode based on organic material. *Microelectronic Engineering*, *85*, 1647-1651. https://doi.org/10.1016/j.mee.2008.04.003

Kaleli, M., Parlak, M., & Erçelebi, Ç. (2011). Studies on device properties of an n-AgIn5Se8/p-Si heterojunction diode. *Semiconductor Science and Technology*, *26*(105013), 1-7. https://doi.org/http://dx.doi.org/10.1088/0268-1242/26/10/105013

Karataş, Ş. (2010). Effect of series resistance on the electrical characteristics and interface state energy distributions of Sn/p-Si (MS) Schottky diodes *Microelectronic Engineering*, *87*, 1935-1940. https://doi.org/10.1016/j.mee.2009.11.168

Karataş, Ş., Altındal, Ş., Türüt, A., & Çakar, M. (2007). Electrical transport characteristics of Sn/p-Si schottky contacts revealed from I–V–T and C–V–T measurements. *Physica B*, *392*, 43-50. https://doi.org/doi:10.1016/j.physb.2006.10.039

Kaya, İ., Kolcu, F., Demiral, G., Ergül, H., & Kiliç, E. (2015). Synthesis and characterization of imine polymers of aromatic aldehydes with 4-amino-2-methylquinoline via oxidative polycondensation. *Designed Monomers and Polymers*, *18*(1), 89-104. https://doi.org/10.1080/15685551.2014.971395

Nallathambi, P., Lal, S. K., Boopalakrishnan, G., Kumar, A., Umamaheswari, C., Gogoi, R., Yadav, S. K., Gupta, A., Meshram, N. M., & Ilangovan, R. (2018). Scanning Electron Microscopy and PCR based methods for detection of False Smut [Ustilaginoidea virens (Cooke) Takahashi] Chlamydospores associated with Rice (Oryza sativa) seeds. *Vegetos*, *31*(1), 20-27. https://doi.org/http://dx.doi.org/10.5958/2229-4473.2018.00003.4

Olusola, O. I., Salim, H. I., & Dharmadasa, I. M. (2016). One-sided rectifying p–n junction diodes fabricated

from n-CdS and p-ZnTe:Te semiconductors. *Mater. Res. Express*, *3*(095904), 1-15. https://doi.org/10.1088/2053-1591/3/9/095904

Ramaiah Subba Kodigala, P. R. D., Hill A.E., Tomlinson R.D., Bhatnagar A.K. (2001). Structural and optical investigations on CdS thin films grown by chemical bath technique. *Materials Chemistry and Physics*, *68*, 22-30.

Reddy, T. S., & Kumar, M. C. S. (2016). Effect of substrate temperature on the physical properties of co-evaporated Sn2S3 thin films. *Ceramics International*, *42*(10), 12262-12269. https://doi.org/10.1016/j.ceramint.2016.04.172

Rocha, F. S., Gomes, A. J., Lunardi, C. N., Kaliaguine, S., & Patience, G. S. (2018). Experimental Methods in Chemical Engineering: Ultraviolet Visible Spectroscopy—UV-Vis. *The Canadian Journal of Chemical Engineering*, *96*, 2512-2517. https://doi.org/10.1002/cjce.23344

Yakuphanoglu, F. (2007). Electrical characterization and interface state density properties of the ITO/C-70/Au Schottky diode. *Journal of Physical Chemistry C*, *111*(3), 1505-1507. https://doi.org/10.1021/jp066912q